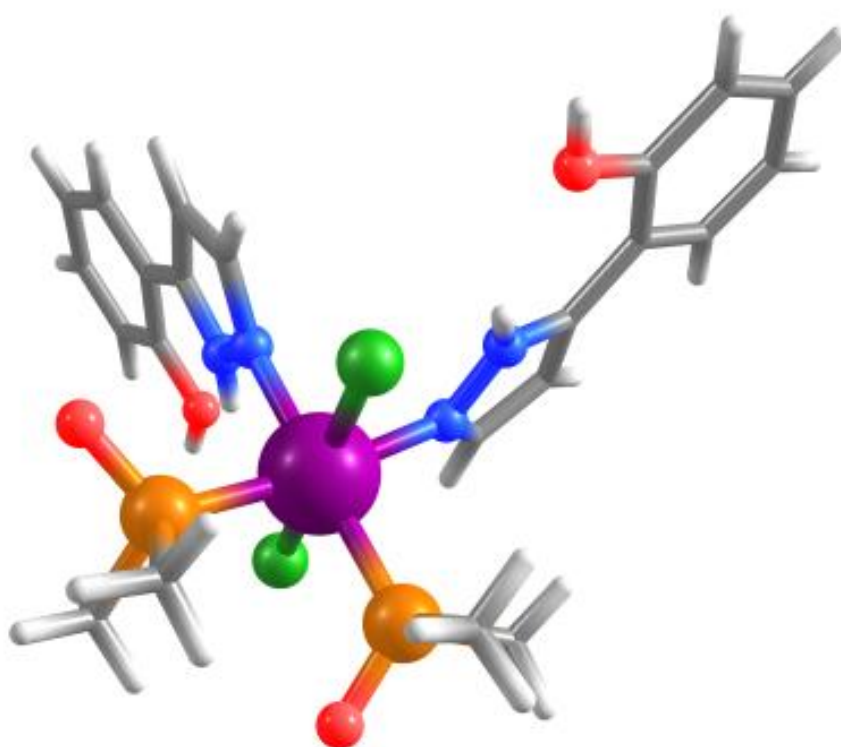# SYNTHESIS OF NEW RU(II) COMPLEXES CONTAINING DMSO AND N-DONOR LIGANDS AS CATALYSTS FOR NITRILE HYDRATION

Lorena Capdevila Güell
Àrea de Química Inorgànica
Memòria del Treball Final de Grau

Index

Resum

Gràcies a l'experiència del grup de recerca en la síntesi de complexos de ruteni amb lligands de tipus dmso i N-donors i la seva aplicació en catàlisi, en aquest treball s'han desenvolupat nous complexos de ruteni utilitzant diferents lligands N-donors i posteriorment s'han avaluat com a catalitzadors per la hidròlisi de nitrils.

Primer de tot s'han sintetitzat dos nous complexos de ruteni (**[2]** i **[3]**) amb un o dos lligands de tipus pzph-OH i un complex de ruteni (**[4]**) utilitzant el lligand terpiridina, en tots els casos amb lligands de tipus dmso i Cl. Els complexos s'han caracteritzat utilitzant diferents tècniques tant espectroscòpiques com electroquímiques.

Pel que fa a la caracterització estructural, s'ha demostrat la formació d'un sol isòmer per als complexos **[2]** i **[3]**. Cal destacar que en el cas del complex **[2],** s'ha obtingut l'estructura cristal·lina que s'ha resolt per difracció de Raig-X. La caracterització del complex **[4]** també s'ha dut a terme per a un dels isòmers que s'ha pogut obtenir pur. Cal mencionar que en aquest cas, s'observa la formació d'un segon isòmer a temps de reacció més llargs.

S'han realitzat espectres UV-Vis en metanol per als complexos **[2]** i **[3]** i diclormetà en el cas del complex **[4]**, on s'ha evidenciat tant la presència de bandes MLCT com també bandes π-π*dels lligands en tots tres casos, i s'han pogut calcular els seus coeficients d'extinció. Els complexos **[2]** i **[3]** presenten un desplaçament de les bandes al llarg del temps, possiblement causat per una substitució d'un lligand per metanol.

Posteriorment, s'han estudiat les propietats electroquímiques dels tres complexos a partir de voltametria cíclica (CV). En el complex **[2]** s'ha observat una ona reversible corresponent al parell redox Ru(III/II) del complex. En canvi, el complex **[3]** exhibeix una ona irreversible degut a un procés d'isomerització d'enllaç Ru-dmso. Per evidenciar aquest fet, s'ha portat a terme un estudi electroquímic d'aquests dos complexos, on s'ha confirmat que el procés d'isomerització d'enllaç el mostra només el complex **[3]**. Per altra banda, també s'ha realitzat la CV del complex **[4]**, que exhibeix una ona reversible observant també una segona ona a temps de reacció més llargs fent evident un cop més la formació d'un segon isòmer.

Per últim, s'ha avaluat l'activitat catalítica en la hidròlisi de nitrils dels complexos **[3]** i **[4]** utilitzant dos substrats diferents, obtenint-se conversions entre moderades i altes per als dos catalitzadors i mostrant excel·lents selectivitats per l'amida.

Resumen

Gracias a la experiencia del grupo de investigación en la síntesis de complejos de rutenio con ligandos de tipo dmso y N-donores y su aplicación en catálisis, en este trabajo, se han desarrollado nuevos complejos de rutenio utilizando ligandos N-donores y posteriormente se ha evaluado como catalizadores par la hidrólisis de nitrilos.

En primer lugar se han sintetizado dos nuevos complejos de rutenio (**[2]** y **[3]**) con uno o dos ligandos de tipo pzph-OH y un complejo de rutenio (**[4]**) utilizando el ligando terpiridina, en todos los casos con ligandos de tipo dmso y Cl. Los complejos se han caracterizado utilizando diferentes técnicas tanto espectroscópicas como electroquímicas.

En cuanto a la caracterización estructural, se ha demostrado la formación de un solo isómero para los complejos**[2]** y **[3]**. Hay que destacar que en el caso del complejo **[2]**, se ha obtenido una estructura cristalina que se ha resuelto por difracción de Rayos-X. La caracterización del complejo **[4]** también se ha llevado a cabo para uno de los isómeros que se ha podido obtener puro. Cabe mencionar que en este caso, se observa la formación de un segundo isómero a tiempos de reacción más largos.

Se han realizado espectros UV-Vis en metanol para los complejos **[2]** y **[3]** y diclormetano en el caso del complejo **[4]**, donde se ha evidenciado tanto la presencia de bandas MLCT como bandas π-π * de los ligandos en los tres casos, y se han podido calcular sus coeficientes de extinción. Los complejos **[2]** y **[3]** presentan un desplazamiento de las bandas a lo largo del tiempo, posiblemente causada por una sustitución de un ligando por metanol.

Posteriormente, se han estudiado las propiedades electroquímicas de los tres complejos a partir de voltametría cíclica (CV). En el complejo **[2]** se ha observado una onda reversible correspondiente a la pareja redox Ru(III/II) del complejo. En cambio, el complejo **[3]**, exhibe una onda irreversible debido a un proceso de isomerización de enlace Ru-dmso. Para evidenciar este hecho, se ha llevado a cabo un estudio electroquímico de estos dos complejos, donde se ha confirmado que el proceso de isomerización de enlace lo muestra sólo el complejo **[3]**. Por otra parte, también se ha realizado la CV del complejo **[4]**, que exhibe una onda reversible observando también una segunda onda en tiempo de reacción más largos haciendo evidente una vez más la formación de un segundo isómero.

Por último, se ha evaluado la actividad catalítica en la hidrólisis de nitrilos de los complejos **[3]** y **[4]** utilizando dos sustratos diferentes, obteniéndose conversiones entre moderadas y altas para los dos catalizadores y mostrando excelentes selectividades por la amida.

Summary

Thanks to the experience of the research group in the synthesis of ruthenium complexes with dmso and N-donor ligands and their application in catalysis, in this work we have developed new ruthenium complexes using N-donor ligands that have been subsequently evaluated as catalysts for the nitrile hydrolysis reaction.

First, two new ruthenium complexes ([2] and [3]) with one or two pzph-OH ligand have been synthesized, together with a ruthenium complex ([4]) with the terpyridine ligand, in all cases with dmso and Cl ligands. The complexes have been characterized using different spectroscopic and electrochemical techniques.

With respect to structural characterization, the formation of a single isomer for [2] and [3] complexes has been shown. It should be noted that in the case of complex [2] the crystal structure has been obtained that has been solved by X-ray diffraction analysis. The characterization of complex [4] has also been carried out for one of the isomers that has been obtained in pure form. It should be mentioned that in this case, it is observed the formation of a second isomer for longer reaction times.

UV-Vis spectra have been performed in methanol for complexes [2] and [3] and dichlormetane for the [4] complex, where the presence of MLCT and intraligand π-π * bands it evidenced in the three cases, and the corresponding extinction coefficients could be calculated. For complexes [2] and [3] a wavelength shift along the time is observed, possibly due to exchange of one ligand by methanol.

Subsequently, the electrochemical properties of the three complexes have been studied by cyclic voltammetry (CV). For complex [2], a reversible wave corresponding to the Ru(III/II) redox pair has been observed. On the contrary, complex [3] exhibits an irreversible wave due to a Ru-dmso bond isomerization process. To demonstrate this fact, an electrochemical study of the two mentioned complexes has been carried out, which has cofirmed that the isomerization process is shown only by complex [3]. Moreover, we also registered the CVs for complex [4], which exhibits a reversible wave; a second wave was observed for longer reaction times evidencing once again the formation of a second isomer.

Finally, the catalytic activity in the hydrolysis of nitriles of the complex [3] and [4] has been evaluated using two different substrates, obtaining moderate to high conversions and excellent selectivity for the amide product.

Abbreviations

Anal. Found (Calc.)	analysis found (analysis calculated)
CH_3CN	Acetonitrile
COSY	correlation spectroscopy
CV	cyclic voltammetry
d	Doblet
dd	double doblet
dmso	dimethyl sulfoxide
ε	extinction coefficient
$E_{1/2}$	half wave potential
$E_{p,a}$	Anodic peak potential
$E_{p,c}$	Cathodic peak potential
ESI- MS	electrospray ionization mass spectrometry
GC	gas chromatography
IR	Infrared
ml	Milliliters
MLCT	metal to ligand charge transfer
mmol	Milimol
m/z	mass-to-charge ratio
NMR	nuclear magnetic resonance
NOESY	nuclear Overhauser effect spectroscopy
T	Triplet
TBAH	tetra(n-butyl)ammonium hexafluorophosphate
Td	Triplet doble
terpy	2,2`:6',2''-terpyridine
ν	Frequency
Λ	Wavelength

1. Introduction

1.1 Ruthenium core concepts

The study of ruthenium complexes is of high interest due to their applications in different fields of science.[1] Ruthenium is a metal situated in the d group of the periodic table whose electronic configuration is [Kr] $4d^7 5s$. One relevant feature for this element together with the osmium, is the diversity of the oxidation states that can display its complexes (from -2 in $[Ru(CO)_4]^{2-}$] to +8 in $[RuO_4]$). In addition, it can present several coordination geometries (trigonal bipyramid, octahedral...).

The ruthenium complexes are particularly interesting because of their kinetic stability in different oxidation states, the reversible nature of the redox pairs and their synthetic simplicity. On the other hand, these compounds are characterized for their high electron transfer capacity,[2,3] their relatively low redox potential values and their ability to stabilize reactive metallic species as oxo-metal [4] and also metal-carbene complexes. [5]

The properties and applications of ruthenium complexes are characterized for the nature of the ligand coordinated to the central metal. So the organometallic compounds with π-conjugated ligands or another type of ligands that allow the electronic delocalization have shown specific properties in nonlinear optics,[6] magnetism,[7] molecular sensors [8] and liquid crystals.[9] Moreover, complexes with heterocyclic N-donor ligands are the most used thanks to their interesting spectroscopic, photophysical and electrochemical properties. [10] This fact gives rise a several applications in a wide area such as molecular electronic devices,[11] and photoactive DNA cleavage agents for therapeutic purposes and others.[12]

1.2 Ruthenium complexes with sulfoxide ligands

The study of the transition metal complexes with sulfoxide ligands has increased rapidly after the first article reported in the sixties.[13] One relevant feature that makes this complexes interesting is their use as precursors for the synthesis of a wide range of organometallic and coordination compounds,[14] and their application in a high number of catalytic processes.[15] It should be noted their utility in medical chemistry as antitumor and antimetastatic agents.[16] From a chemical viewpoint, these compounds are very interesting due to bond isomerization linkage process thanks to the ambidentate behavior of sulfoxide ligand.

1.2.1 Ru-dmso bond

As mentioned above, the ambidentate nature of this ligand is a relevant characteristic of these complexes given its potential coordination through the O atom or the S atom. This fact depends on different factors such as the metal properties, the rest of the ligands coordinated on the metal and also steric impediments. Normally the dmso ligand coordinates to the metal through the O atoms. However, the coordination through the S atom occurs in metals in the group VIII, usually those of the second and third transition groups, as is the case of ruthenium. This type of ligand, can coordinate to ruthenium through the S and also the O atom. For example the Ru^{II} oxidation state (d^6 low spin configuration) has more affinity to S atom given its character of soft Lewis acid. In contrast, for Ru^{III} (d^5 low spin configuration) the coordination via O atom is favored due to the harder Lewis acid nature.
.

Consequently, the Ru-dmso complexes can suffer bond (linkage) isomerization processes. There are some factors that can lead to this isomerization:

- ✓ Changes in metal oxidation state: $[Ru^{II}(NH_3)_5(S\text{-}dmso)]^{2+}$ or $[Ru^{III}(NH_3)_5(O\text{-}dmso)]^{3+}$.
- ✓ Coordination of π-acceptor ligands (such as CO or CN) in *trans* to S-dmso ligands.
- ✓ External factors for example temperature or photochemistry.

a) Ru-dmso coordination through sulphur

In accordance with the Pearson acid-base theory, [17] diffuse orbitals from metallic ions are overlapped with donor diffuse orbitals from S. Due to the π-acceptor properties of the dmso ligand, the metal-S bond is favored because of π -retrodonation from metal to dmso orbitals. Ru(II) is an example of this fact, where Ru-S linkage is stabilized by transferring π electronic density from the metal to the empty orbitals of the dmso ligand. This bond presents a certain character of double bond caused by this π-retrodonation. In consequence, it can be observed that the average Ru-S distances are lower than the sum of the covalent radius. When the Ru(II) is oxidated to Ru(III), it is observed a decrease of the π retrodonation and the Ru-S distances increase.

In complexes with two dmso ligands in *trans* position, the Ru-S bond distances increase, suggesting a bond order reduction because of competition of the π electronic density of the metal between the two dmso ligands. This effect is also evident in reactions between Ru(II)-dmso complexes and π-acceptor ligands such as CN or CO provoking a linkage bond isomerization.

### b) Ru-dmso coordination through oxygen

When the dmso ligand is coordinated to metal through oxygen atom (from Ru-S to Ru-O), it is observed a decrease of the bond order in the S-O linkage. Consequently, in general there is an increase of the bond distance. For hard metallic ions (such as Ru(III)), the bond $Ru\text{-}O_{dmso}$ is favored. In contrast, for the soft metallic ions (Ru(II)), this $Ru\text{-}O_{dmso}$ coordination mode can take place in order to avoid the *trans* disposition of two S-dmso as well as by the presence of π-acceptor ligands (CO,CN).

1.3 Ruthenium-dmso complexes as catalysts

As mentioned above, the ruthenium complexes present several applications in the catalytic field, since they can catalyze a wide range of reactions including reductive and oxidative processes. In this work, the research is centered to study new ruthenium complexes with dmso ligands and their application such as catalyst in the hydrolysis of nitrile.

1.3.1 Hydrolysis of nitrile

The nitrile hydrolysis is a reaction very interesting from the industrial and pharmacological point of view because it leads to the synthesis of amides (for example the acrylamide and benzamide) as well as carboxylic acid from the corresponding nitriles (Scheme 1).
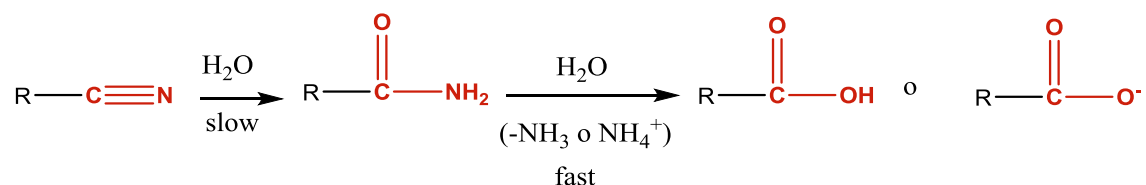
Scheme 1: Nitrile hydrolysis reaction to obtain the amide and further transformation to carboxylic acid.

Originally, this reaction was catalyzed by strong acids and bases. However, these conditions showed some disadvantages like:

- Formation of salts after the final neutralization of the medium causing their removal difficult.
- Control of the temperature and reagents to avoid overheating and polymerizations.
- Waste generated (pollutants).
- Low selectivity for the amide due to the fast hydrolysis to carboxylic acid.

For those exposed drawbacks, is necessary to find a method with a better yield for the amide products. For this reason, the metal catalyst was introduced in this reaction in order to activate the nitrile group and so reduce the drawbacks mentioned above.

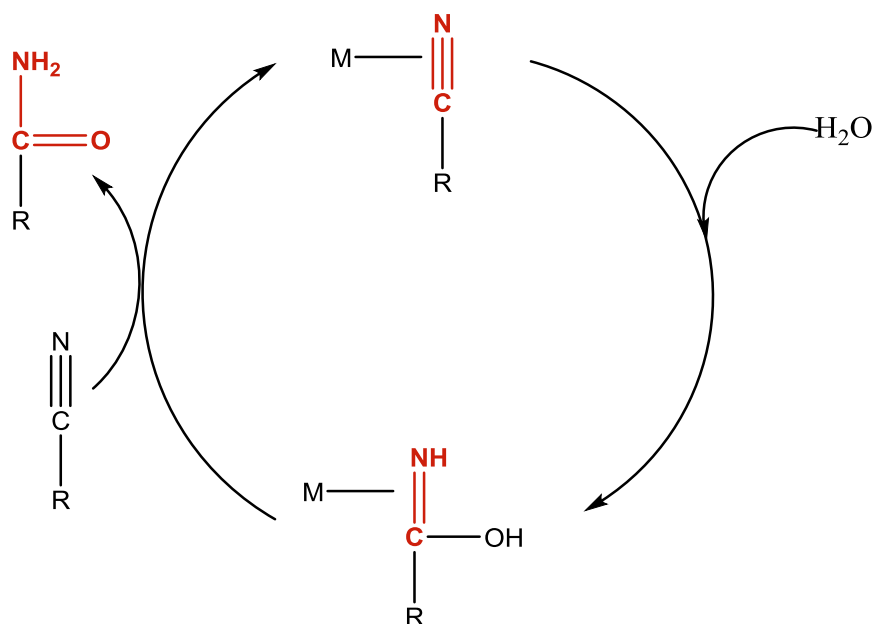### a) Nitrile hydrolysis reaction mediated by metallic ions

Thanks to the presence of metallic ions in this reaction, the amide can be obtained more selectively at softer reaction conditions. The metallic center activates the CN bond, increasing significantly the reaction rate.

In Scheme 2 the reaction of hydrolysis of nitrile groups mediated by metals is described, where a nucleophilic attack of a OH⁻ group takes place thanks to the activation provided by coordination of the nitrile N atom to the metal.
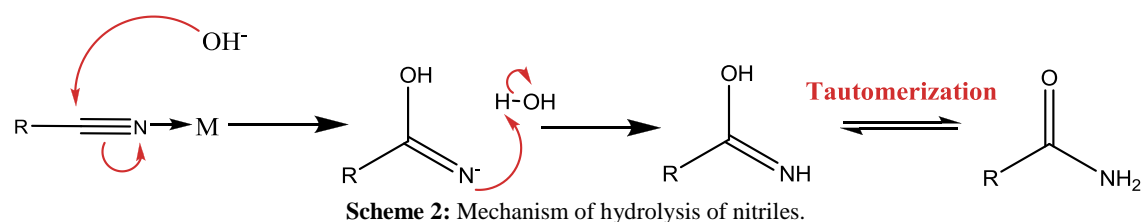
Scheme 2: Mechanism of hydrolysis of nitriles.

A catalytic cycle is proposed, where there is a rapid replacement of the coordinated amide by nitrile, repeating successively (Scheme 3).[18]

Scheme 3: Catalytic cycle of the nitrile hydrolysis reaction in presence of a metal catalyst.

The first metal catalysts were hydride-type such as the Ru-dihydrocomplexes of Murahashi $[RuH_2(PPh_3)_4]$ [19] or the Pt-hydrocomplex of Parkins $[PtH(PMe_2OH)\{(PMe_2O)_2H\}]$. [20] Later, acetylacetone complexes as *cis*-$[Ru(acac)_2(PPh_2py)_2]$ [21] and Rh(I) organometallics as the systems $[\{Rh-(m-OMe)(cod)\}_2]/PCy_3$ (cod = 1,5-cyclooctadiene, Cy = cyclohexyl) were developed. [22] Using these complexes avoids the disadvantages stated above but the problem is that organic solvents are used as reaction medium and these are polluting for the environment.

Cadierno and co-workers developed nitrile hydrolysis protocols in pure water under neutral conditions using ruthenium (II)-arenes and bis(allyl)-ruthenium(IV) with P-donor ligands as catalysts, giving high yields and selectivity to amide. [23] However, there are only few reports on Ru complexes containing N-donor O-donor and dmso ligands applied to this process.

2. Objectives

As mentioned in the introduction, the hydrolysis of nitriles is a reaction of great interest from an industrial and pharmacological perspective. On the research group where this TFG has been developed one of the research lines involves the study of ruthenium complexes with N or S-donor ligands[24] for the hydrolysis of nitriles. The general objectives of this work were the design of new ruthenium complexes with dmso and different types of N- and O-donor ligands and the evaluation of these complexes as catalyst for the nitrile hydrolysis reaction.

The specific objectives are:

- Synthesis and characterization of new ruthenium complexes with ligands of type chlorido, dmso and pzph-OH (Scheme 5).

- Synthesis and characterization of ruthenium complexes with chlorido, dmso and terpyridine ligands.

- Evaluation of the catalytic activity of all complexes synthesized for the nitrile hydrolysis reaction.

3. Experimental section

3.1 Instrumentation and measurements

- *UV-VIS*

UV-Vis spectroscopy was performed on a Cary 50 Scan (Varian) UV-Vis spectrophotometer with 2 mm quartz cells.

- *Cyclic voltammetry*

CV and DPV experiments were performed in an IJ-Cambria IH-660 potentiostat using a three electrode cell. Glassy carbon electrode (3 mm diameter) from BAS was used as working electrode, platinum wire as auxiliary and $Ag/AgNO_3$ or $Ag/AgCl$ as the reference electrode. The complexes were dissolved in solvents containing the necessary amount of n-Bu_4NPF_6 (TBAH) as supporting electrolyte to yield a 0.1 M ionic strength solution. All $E_{1/2}$ values reported in this work were estimated from cyclic voltammetric experiments as the average of the oxidative and reductive peak potentials $(E_{p,a}+E_{p,c})/2$, or directly from DPV peaks.

- IR

IR spectroscopy was performed on an Agilent Technologies, Cary 630 FTIR equipped with an ATR system, directly on the samples without any previous treatment.

- *^{1}H-NMR*

The ^{1}H-NMR spectroscopy was performed on a Bruker DPX 400 MHz. Samples were run in acetone-d_6 or $CDCl_3$ with internal references (residual protons and/or tetramethylsilane).

- *Elemental analyses*

Elemental analyses were performed using a ESI-MS. CHNS-O Elemental Analyser EA-1108 from Fisons.

- *Gas chromatography*

Gas chromatography experiments were performed by capillary GC, using a GC-2010 Gas Chromatograph from Shimadzu, equipped with an Astec CHIRALDEX G-TA Column (30 m x 0.25 mm diameter) incorporating a FID detector. All the product analyses in the catalytic experiments were performed by means of calibration curves using biphenyl as internal standard.

- *X-Ray diffraction analyses*

The measurement was carried out on a *BRUKER SMART APEX CCD* diffractometer using graphite-monochromated Mo $K\alpha$ radiation (λ = 0.71073 Å) from an x-Ray Tube. The measurements were made in the range 2.202 to 28.666° for θ. Full-sphere data collection was carried out with ω and φ scans. Programs used: data collection, Smart[25]; data reduction,

Saint+;[26] absorption correction, SADABS.[27] Structure solution and refinement was done using SHELXTL.[28] The structure was solved by direct methods and refined by full-matrix least-squares methods on F^2. The non-hydrogen atoms were refined anisotropically. The H-atoms were placed in geometrically optimized positions and forced to ride on the atom to which they are attached.

3.2 Synthesis of the compounds

Synthesis of [RuCl$_2$(dmso)$_4$], [1]

The ligand 2-(1H-pyrazol-3-yl)phenol, pzph-OH,[29] and the complex [RuCl$_2$(dmso)$_4$], [1],[30] were prepared according to the procedure described in the literature, which is detailed below for complex [1]:

A 1 g (3.83 mmol) of RuCl$_3$·2.38H$_2$O was refluxed in 5 mL of dmso and it was added two drops of H$_2$O at 170 °C for 10 minutes. After this time, the solution was cooling to room temperature; 10 mL of acetone was added. The yellow precipitate formed was separated by filtration and successively washed with acetone and ether and dried in vacuum. Yield: 214.8 mg (11%). $E_{p,a}$ (CH$_2$Cl$_2$ + 0.1 M TBAH): 1.38 V vs. Ag$^+$/AgCl.

Synthesis of [RuCl$_2$(dmso)$_2$(pzph-OH)$_2$], [2] and [RuCl$_2$(dmso)$_3$(pzph-OH)], [3]

A mixture of [RuCl$_2$(dmso)$_4$] (76.8 mg, 0.15 mmol), and pzph-OH (25.4 mg, 0.15 mmol) in nitrogen-degassed CH$_2$Cl$_2$ (4 mL) were refluxed at 40 °C for 90 minutes. The mixture was cooled to ambient temperature. The yellow precipitate obtained, which corresponds to compound [2], was recovered with a glass frit and was dried under vacuum. Yield: 27.3 mg (27%). Posteriorly, a solid mixture of [2] and [3] was obtained by adding ether to the solution obtaining a precipitate that was filtered. The mixture was purified by further recrystallization in CH$_2$Cl$_2$/ether mixtures. A green solid was obtained which corresponds to compound [3]. Yield: 35.3 mg (45%).

For [2], ^{1}H-NMR (400 MHz, acetone d$_6$): δ = 3.14 (s, 12H, H9), 6.80 (d, 2H, H8, J_{H8-H3} = 2.14 Hz), 6.93 (td, 2H, H7, $J_{H7-H4,5}$ = 7.08, Hz, J_{H7-H6} = 1.07 Hz), 7.07 (dd, 2H, H6, J_{H6-H5} = 8.12 Hz, J_{H6-H7} = 1.26 Hz), 7.21 (td, 2H, H5, $J_{H5-H6,H7}$ = 7.93 Hz, J_{H5-H4} = 1.66 Hz), 7,68 (dd, 2H, H4, J_{H4-7} = 7.93 Hz, J_{H4-H5} = 1.70 Hz), 8.09 (d, 2H, H3, J_{H3-H8} = 2.23 Hz), 9.89 (s, 2H, H2), 13.41 (s, 2H, H1). For the NMR assignation we have used the numbering scheme shown in Figure 3. IR (cm^{-1}): υ = 3260 (υ (OH)); 3050 (υ (NH)); 1606 (υ (C-N)sp^2); 1442 (υ (C-C)sp^2) 1064 (υ (S=O)). $E_{1/2}$ Ru(III/II) (CH$_3$CN + 0.1 M TBAH): 0.77V vs. Ag$^+$/AgNO$_3$. UV-Vis (MeOH): λ$_{màx}$, nm (ε, M^{-1} cm^{-1}) 270 (17446), 306 (12307). ESI-MS (m/z): 646.8 [M-H]$^-$, 486.7 [M-(pzph-OH)-H$^+$]$^-$.

For [3], ^{1}H-NMR (400 MHz, acetone-d$_6$): δ = 3.20 (s, 6H, H11), 3.46 (s, 6H, H10), 3.49 (s, 6H, H9), 6.86 (d, 1H, H8, J_{H8-H3} = 1.67 Hz), 6.99 (td, 1H, H7, $J_{H7-H5,H4}$ = 8.23 Hz, J_{H7-H6} =0.55 Hz), 7.12 (dd, 1H, H6, J_{H6-H5} = 8.23 Hz, J_{H6-H7} = 0.27 Hz), 7.26 (td, 1H, H5, $J_{H5-H6,H7}$ = 8.23 Hz, J_{H5-H4} = 1.53 Hz), 7.72 (dd, 1H, H4, J_{H4-H7} =7.92 Hz, J_{H4-H5} =1.53 Hz), 8.55 (d, 1H, H3, J_{H3-H8}

=2.69 Hz), 9.68 (s, 1H, H2), 14.36 (s, 1H, H1). For the NMR assignation we have used the numbering scheme shown in Figure 4. Anal Found (Calc.) for $C_{15}H_{26}Cl_2N_2O_4RuS_3 \cdot 1CH_2Cl_2 \cdot H_2O$: C, 28.76 (28.70); N, 3.79 (4.18); H, 4.41 (4.51). IR (cm^{-1}): υ = 3130 (υ (OH)); 3010 (υ (NH)); 1594 (υ (C-N)sp^2); 1404 (υ (C-C)sp^2); 1065 (υ (S=O)). $E_{p,a}$ (Ru(II/III) (CH$_3$CN + 0.1 M TBAH): 1.04 V vs. Ag/AgNO$_3$. UV- Vis (MeOH): $\lambda_{màx.}$ nm (ϵ, M^{-1} cm^{-1}) 264 (15838), 297 (8983). ESI-MS (m/z): 564.7 [M-H$^+$]$^-$, 486.7 [M-(dmso)-H$^+$]$^-$, 408.7 [M-2dmso-H$^+$]$^-$.

Synthesis of *cis*-[Ru(2,2':6',2''-terpyridine)(dmso)Cl$_2$], [4]:

The complex *cis*-[Ru(2,2':6',2''-terpyridine)(dmso)Cl$_2$] was prepared through a modification of the procedure described in the literature[31], which is detailed below:

A 137.8 mg (0.28 mmol) of RuCl$_2$(dmso)$_4$, [1], and 67.3 mg (0.28 mmol) of 2,2';6`,2``-terpyridine was heated at 50ºC in 30 mL of CH$_2$Cl$_2$ under nitrogen atmosphere for 6 h. After the reaction time, the solution was cooled and the solvent was partially removed under reduced pressure, and a black solid appeared. It was filtered and washed with Et$_2$O. Finally it was dried under vacuum. Yield: 4 mg (2.9 %). **^{1}H-NMR (400 MHz, CDCl$_3$):** δ = 9.37 (d, 2H, H1, $^3J_{H1-H2}$ = 6.28 Hz), 8.15 (d, 2H, H4, $^3J_{H4-H3}$= 8.17 Hz), 8.10 (d, 2H, H5, $^3J_{H5-H6}$=8.17 Hz), 7.96 (t, 1H, H6, $^3J_{H6-H5}$= 8.17Hz), 7.81 (td, 2H, H2, $^3J_{H2-H1,H3}$= 7.84 Hz, $^4J_{H2-H4}$ = 1.68 Hz), 7.42 (td, 2H, H3, $^3J_{H3-H2,H4}$= 7.39 Hz, $^4J_{H3-H1}$ = 1.68 Hz), 3.77 (s, 6H, H7). For the NMR assignation we have used the numbering scheme shown in Figure 5. UV-Vis (CH$_2$Cl$_2$): $\lambda_{màx.}$ nm (ϵ, M^{-1} cm^{-1}) 272 (12690), 327 (19319), 386 (2919), 518 (3137), 670 (1133). $E_{1/2}$ (Ru(III/II) (CH$_2$Cl$_2$ + 0.1 M TBAH): 0.74 V vs. Ag$^+$/AgCl.

Catalytic experiments

These experiments have been carried out using several nitrile substrates under neutral conditions in water as a solvent at 80ºC. They have been performed using a ratio 0.01mmol:1mmol ([Ru-Catalyst:Substrate]). The remaining substrate has been quantified through GC analysis and employing biphenyl as an internal standard and the selectivities have been analyzed by NMR spectroscopy on the reaction crude as detailed below.
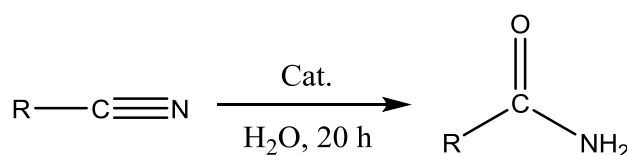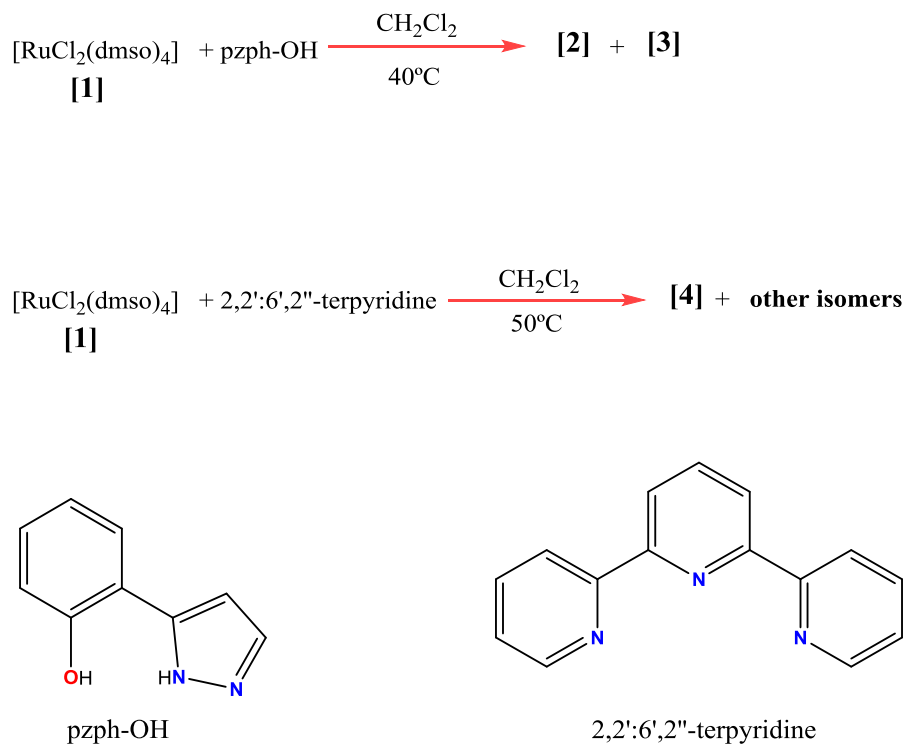

Scheme 4: Nitrile hydrolysis reaction.

A 0.01 mmol of catalyst was dissolved in 3 mL of water, and 1mmol of the nitrile (benzonitrile or acrylonitrile) was added. The mixture was heated at 80ºC for 20 hours in a sealed tube under stirring. After the reaction time, three different extractions with two mL of chloroform (containing biphenyl as an internal standard) were performed in order to collect the non-reacted nitrile. The organic phase was analyzed by CG determining the nitrile conversion. On the other hand, aqueous phase was remained at room temperature until the water was evaporated. The solid obtained from the aqueous phase was analyzed by NMR spectroscopy in order to determine the selectivity of the final product.

4. Results and discussion
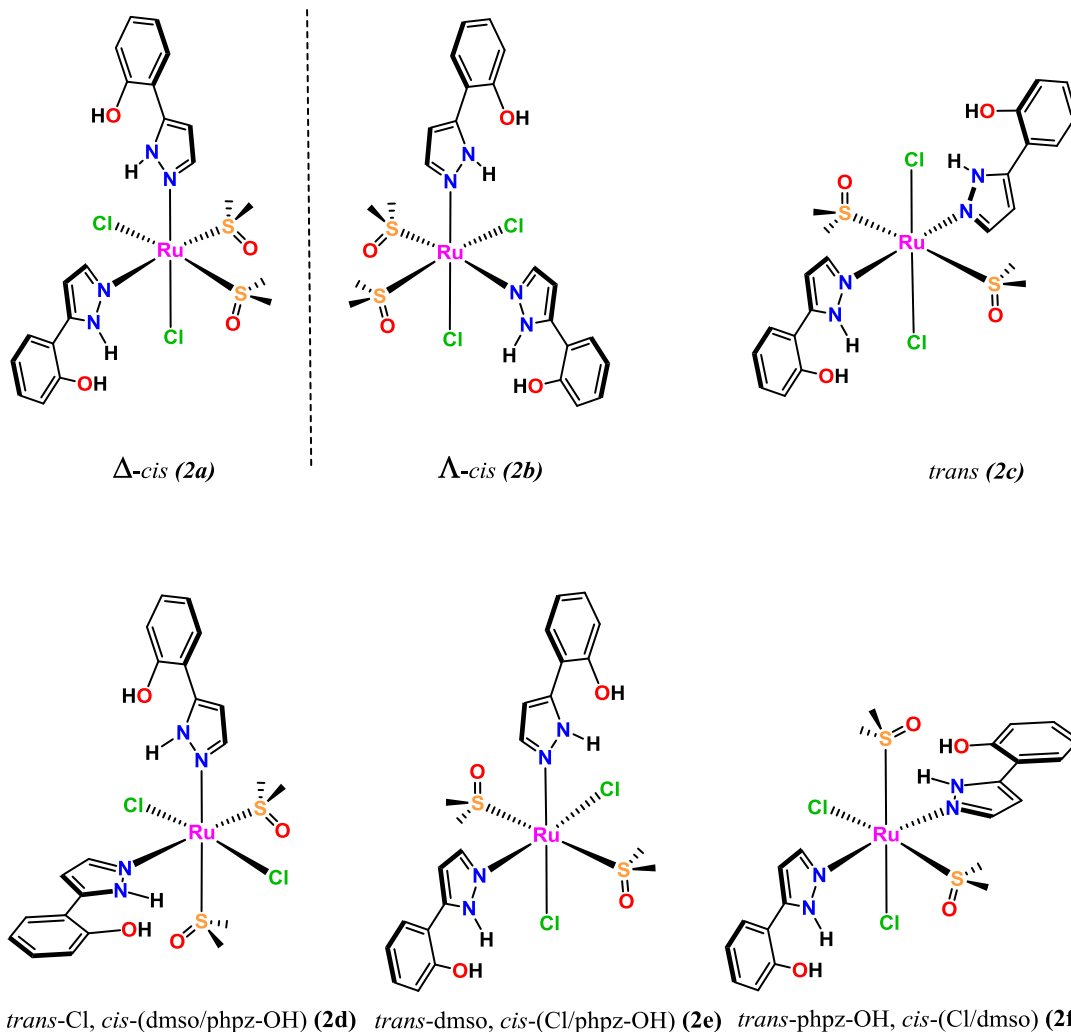
4.1 Synthesis and crystal structures

The schematic syntheses for complexes [**2**], **[3]** and **[4],** together with the ligands used are shown in scheme 5:

$$[RuCl_2(dmso)_4] \; + \; pzph\text{-}OH \; \xrightarrow[40^{\circ}C]{CH_2Cl_2} \; [\textbf{2}] \; + \; [\textbf{3}]$$

[1]

$$[RuCl_2(dmso)_4] \; + \; 2,2'\text{:}6',2''\text{-terpyridine} \; \xrightarrow[50^{\circ}C]{CH_2Cl_2} \; [\textbf{4}] \; + \; \textbf{other isomers}$$

[1]

pzph-OH   2,2':6',2"-terpyridine

**Scheme 5:** Synthetic strategy [2],[3],[4] and ligands used.

The equimolar reaction between **[1]** and pzph-OH ligand at reflux in conduces to a mixture of **[2]** and **[3]** products. The compounds are isolate by their different solubility.

Firstly we obtain complex **[2]** that is less soluble in CH_2Cl_2. In this case, the substitution of two dmso ligands in **[1]** by two pzph-OH ligands can lead to six different stereoisomers, including one pair of enantiomers (Scheme 6). Thanks to the crystal structure (see below) we have observed that the isomer **2d** has formed**.** It seems that **2d** can be favored by the formation of hydrogen bonds between the chloride and $H_{pyrazole}$ atoms. In addition, it is possibly an isomer favored by kinetics factors given that the isomers thermodynamically favored would be **2a**, **2b** and **2f** because they have Cl and dmso ligands coordinated in *trans* position, thanks to synergistic effects among π-donor and π-acceptor capacity of Cl and dmso respectively.[32]

Δ-*cis (2a)*   Λ-*cis (2b)*   *trans (2c)*

trans-Cl, *cis*-(dmso/phpz-OH) **(2d)**   *trans*-dmso, *cis*-(Cl/phpz-OH) **(2e)**   *trans*-phpz-OH, *cis*-(Cl/dmso) **(2f)**

Scheme 6: Possible stereoisomers for complex **[2]**.

On the other hand, complex **[3]** is isolated by ether addition because this complex is more soluble in dichloromethane. Three different isomers can be formed for **[3]** (Scheme 7). A crystal was not obtained for this compound but, thanks to NMR spectra (see below), it can be concluded that the isomer isolated is **3a**, which is favored thanks to the formation of two *trans* Cl-Ru-dmso diagonals. Furthermore the pzph-OH ligand can form hydrogen bonds with the Cl or dmso ligands in *cis*.
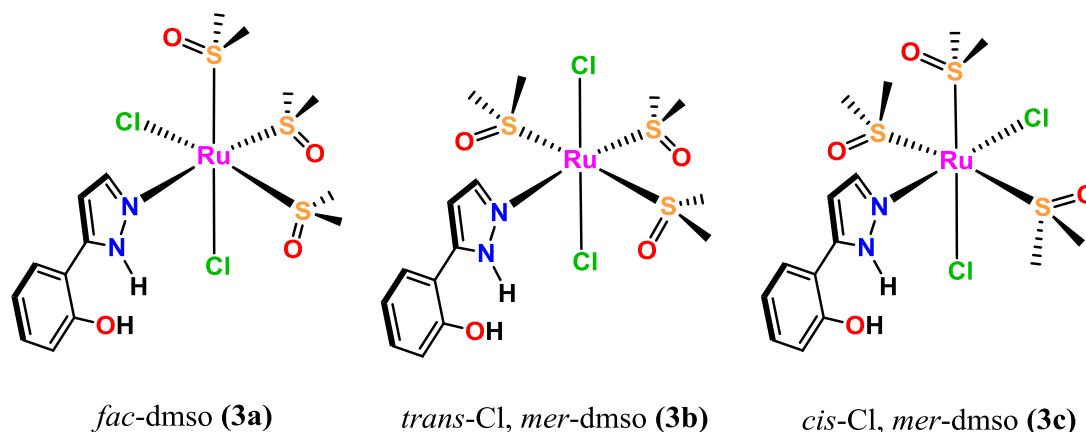
Scheme 7: Possible stereoisomers for complex [3].

As mentioned earlier, the crystal structures of complex [2] has been solved by X-ray diffraction analysis. Figure 1 shows the molecular structure of [2] and their main selected bond lengths and angles can be found in table 1.
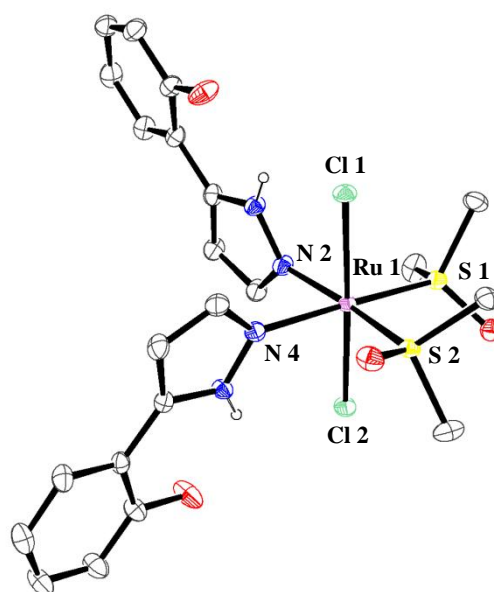

Figure 1: Ortep plot and labeling schemes for compound [2].

In this complex, the Ru metal center adopts an octahedrally distorted type of coordination. Comparing the Ru-N bond lengths with other complexes, where N-donors ligands have a dmso ligand in *trans* position, synthesized in the group, it is observed that the distances are within the expected values for this type of complex.

bond lengths		bond angles	
Ru(1)-N(2)	2.115(5)	N(2)-Ru(1)-N(4)	84.03(18)
Ru(1)-N(4)	2.116(4)	N(2)-Ru(1)-S(1)	92.90(12)
Ru(1)-S(1)	2.2435(14)	N(4)-Ru(1)-S(1)	174.97(12)
Ru(1)-S(2)	2.2489(15)	N(2)-Ru(1)-S(2)	172.68(12)
Ru(1)-Cl(1)	2.3959(14)	N(4)-Ru(1)-S(2)	88.88(13)
Ru(1)-Cl(2)	2.4145(13)	S(1)-Ru(1)-S(2)	94.30(5)
		N(2)-Ru(1)-Cl(1)	88.59(13)
		N(4)-Ru(1)-Cl(1)	89.64(11)
		S(1)-Ru(1)-Cl(1)	86.30(5)
		S(2)-Ru(1)-Cl(1)	93.19(5)
		N(2)-Ru(1)-Cl(2)	89.30(12)
		N(4)-Ru(1)-Cl(2)	88.94(11)
		S(1)-Ru(1)-Cl(2)	95.02(5)
		S(2)-Ru(1)-Cl(2)	88.75(5)
		Cl(1)-Ru(1)-Cl(2)	177.57(5)

Table 1: Select bond lengths (Å) and angles (º) for **[2]**.

It has been registered ESI-MS in mode negative for complexes **[2]** and **[3]**. For **[2]** it is observed one peak with m/z= 646.8 corresponding to the deprotonated complex and another peak at m/z= 486.7 associated to the deprotonated complex without one pzph-OH ligand. On the other hand, for **[3]** a peak at 564.7 is found corresponding to deprotonation of the complex together with two peaks associated with the loss of one or two dmso ligands at m/z= 486.7 and 408.7 respectively.

Figure 2 shows the experimental and calculated isotopic distribution for the molecular (deprotonated) peaks of the complexes.
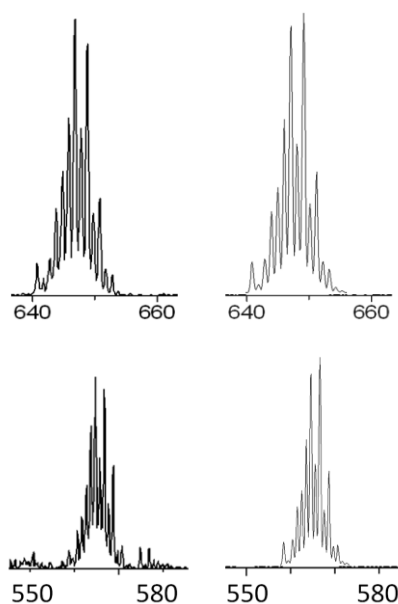

Figure 2: Isotopic distribution for the deprotonated forms of complexes **[2]** (top) and **[3]** bottom in ESI-MS spectra: left, experimental peak and right, calculated.

Initially, it was expected a bidentate coordination of the pzph-OH ligand forming a chelate complex. Thanks to the crystallographic structure obtained for complex **[2]**, we could confirm a metal-ligand coordination in a monodentate manner. In the case of **[3]**, containing only one pzph-OH ligand, the elemental analysis and ESI-MS experiments also point out to a metal-ligand coordination in monodentate form such as complex **[2]**. Probably the ligand deprotonation would assist to its coordination in bidentate manner. To confirm this, a test has been done for complex **[3]**. This complex was dissolved in $CDCl_3$ and then EtONa was added. In NMR spectroscopy analysis it was observed a disappearance of the signals corresponding to the complex and the appearance of one peak at $\delta = 2.5$ ppm corresponding to free dmso. These remarks can be interpreted assuming that the deprotonation of ligand leads to its coordination in bidentate form replacing a dmso ligand, but this process involves the ruthenium oxidation (Ru(II) to Ru(III)), that has paramagnetic behavior.

Complex **[4]** is obtained by an equimolar reaction between **[1]** and the trpy (2,2':6',2''-terpyridine) ligand under heat conditions in CH_2Cl_2 for 6h. In this reaction, two different types of isomers are produced (Scheme 8). It is interesting to note that we have detected a mixture of two different isomers dependently on the refluxing time. It is observed that, when the reaction time is 6 hours, it is obtained only the **4a** isomer. Nevertheless, if the refluxing time is 24 hours, a mixture of **4a** and **4b** isomers is isolated. As happened with complex **[3]**, the formation of a Cl-Ru-dmso diagonal favors the thermodynamic stability of the **4a** isomer respect to **4b** isomer.

cis-Cl, mer-terpy **(4a)**   trans-Cl, mer-terpy **(4b)**
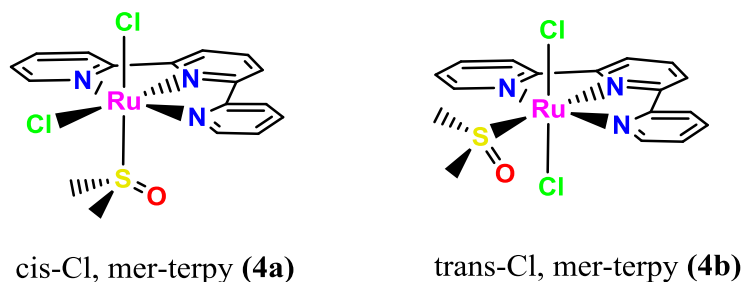
Scheme 8: Possible stereoisomers for complex **[4]**.

4.2 Spectroscopic properties

IR spectra have been registered for **[2]** and **[3]**. The more relevant factor of IR spectra is, in both cases, the absence of any significant vibration in 920-930 cm^{-1} range indicating a sulfur-bonded dmso complex.

For **[2]** and **[3]** complexes the one-dimensional (1D) and two-dimensional (2D) NMR spectra were registered in acetone-d_6 (figures 2 and 3). The one-dimensional (1D) NMR spectra for **[4]** was registered in $CDCl_3$ and is shown in figure 4. All of these complexes manifest two sets of signals: one of them in the aromatic region where the N-donor ligands are observed and the other one in the aliphatic region corresponding to the methyl groups of dmso ligands.

For complexes **[2]** and **[3]**, we can assign all the protons thanks to NOESY and COSY spectra. In the case of **[2]**, which presents a C2 symmetry axis that interconverts all the identical ligands, the two pzph-OH ligands and the two dmso show magnetically equivalent signals. Nevertheless, for compound **[3]** a symmetry plane that contains the pzph-OH ligand and the dmso ligand in *trans* is found. The protons of pyrazole (H8 and H3) have been determined by chemicals shifts

since H3 has a higher chemical shift because it is closer to the N atom of the pyrazole that is a π-acceptor atom. In addition, it is confirmed the assignment of H6, given that it is observed in the NOESY spectra where a NOE appear between H6 and the proton of the alcohol. H1 and H2 are easily identified because both protons are observed at high chemical shift. Given that pyrazolic hydrogen is more acidic than the proton of alcohol, it has been concluded that H1 corresponds to the pyrazolic hydrogen at δ= 13.41 ppm. Therefore the alcohol hydrogen is identified at δ= 9.89 ppm (H2).

On the other hand, the ^{1}H-NMR spectrum for complex **[3]** shows three singlets in the aliphatic region corresponding to the dmso ligands. The dmso that has the pzph-OH ligand in *trans* position, has two methyl groups magnetically equivalent and is identified at 3.49 ppm (H9) because they are closer to two chlorido ligands. Due to the symmetry plane, the two remaining dmso ligands show two resonances: one corresponding to the two methyl groups pointing towards the Cl ligands and the other one assigned to the other two methyl groups. These two signals (H10 and H11) are assigned at 3.46 and 3.20 ppm respectively. The H10 protons are identified at 3.46 ppm because they are closer to Cl ligands producing a deshielding effect.

Moreover, for complex **[4]** all the protons have been assigned thanks to the literature. In ^{1}H-NMR spectra are observed six proton patterns in the aromatic region because of a symmetry plane that contains the two chlorido ligands. The protons with the same multiplicity (for example H1 and H4) have been assigned thanks to the proximity of the N atom, given that a proton closer to the N atom experiments a higher chemical shift. Thanks to ^{1}H-NMR spectra, it has been confirmed that the isomer formed is **(4a)** as it has mentioned above, despite not having the crystal structure. The *cis*-isomer has a higher chemical shift than the *trans*-isomer for the 2-pyridyl protons, given that these protons are closer to a Cl leading to a higher chemical shift.
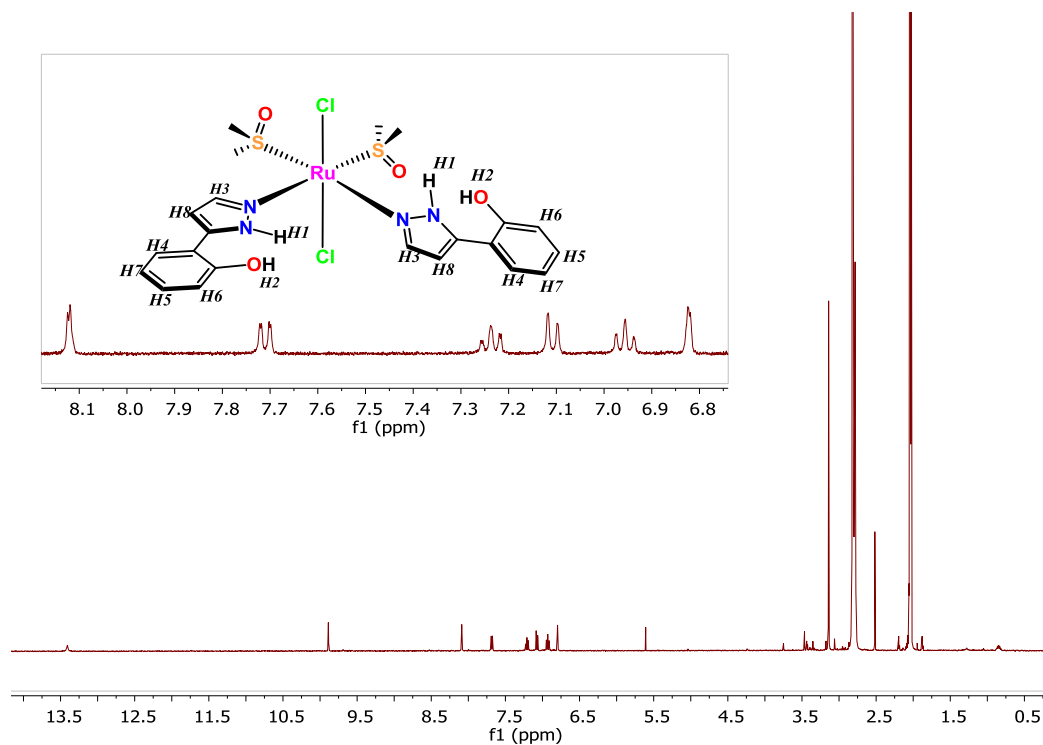

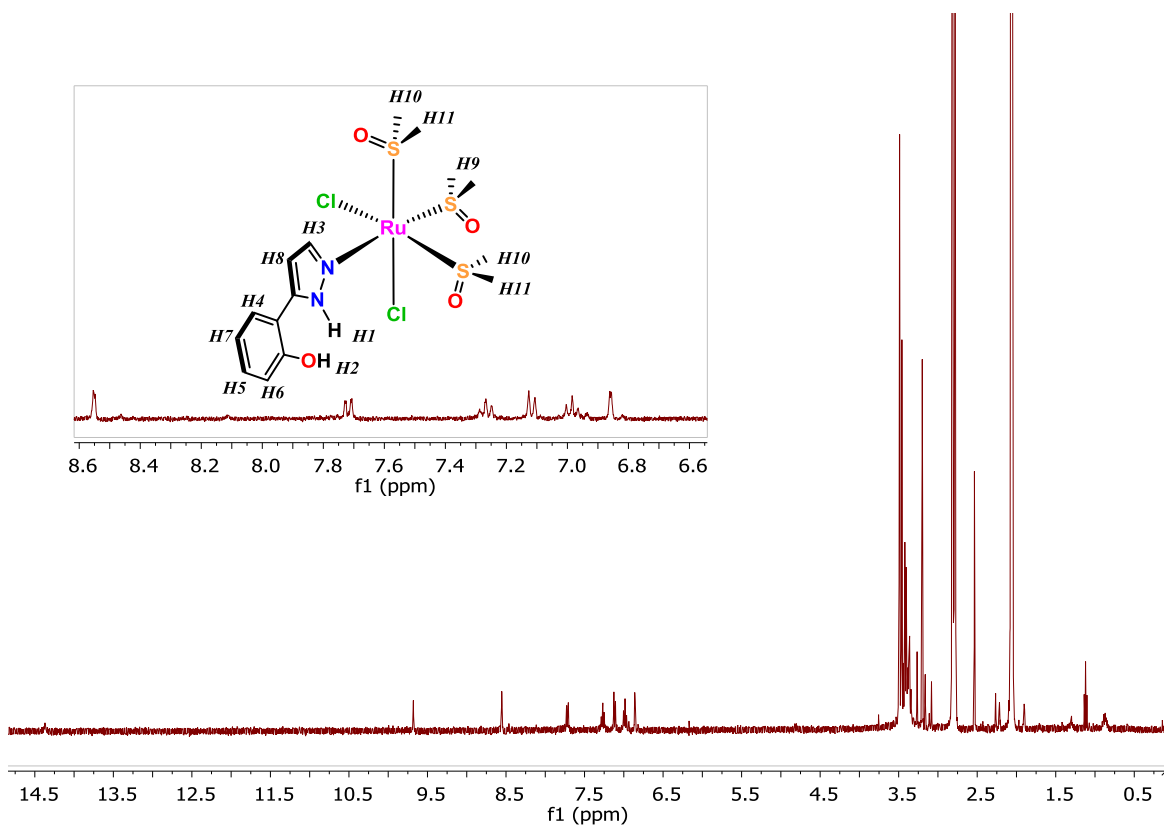**Figure 3**: ^{1}H-NMR spectrum of **[2]**, 400MHz, acetone-d$_6$.

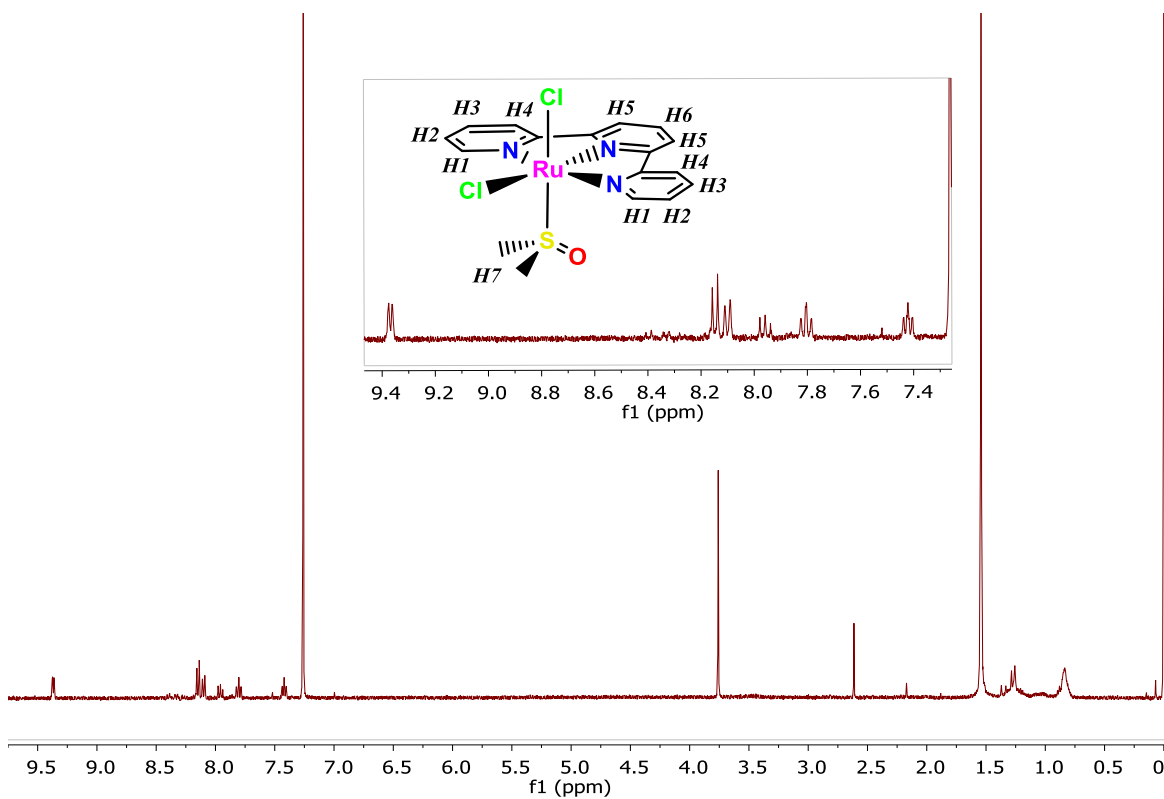**Figure 4:** 1H-NMR spectrum of **[3]**, 400MHz, acetone-d_6.

Figure 5: ^{1}H-NMR spectrum of **[4]**, 400MHz, CDCl$_3$.

The UV-Vis spectra of complexes **[2], [3]** and **[4]** have been performed in CH_3OH (for **[2]** and **[3]**) and CH_2Cl_2 (for **[4]**) and are displayed in Figures 6-8 respectively .The complexes **[2]** and **[3]** exhibit relatively intense bands between 250 and 300 nm assigned to metal-to-ligand $d\pi$-π* charge transfers (MLCT). For complex **[4]**, the same type of absorption bands are found between 450 and 550 nm. All the complexes present intraligand π-π* absorptions at lower wavelengths. As it can be observed, for **[2]** and **[3]** the absorption bands have higher energy than those of **[4]**. This is due to the lower aromatic character of the monodentate pzph-OH ligand compared to terpyridine that provokes a blue-shift of the $d\pi$-π* and intraligand bands for complexes **[2]** and **[3]**.

For complexes **[2]** and **[3]**, UV-Vis spectra have been registered during three consecutive days for the same solution, as it is shown in figures 6 and 7. It has been observed a change of the spectra within 24 h denoting the instability in solution for this complexes. Probably a substitution of a ligand by methanol takes place but further experiments are needed to confirm this point.
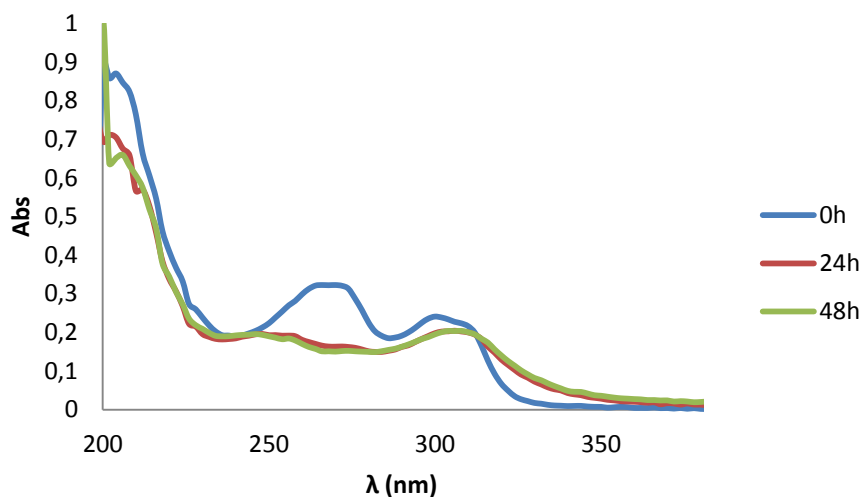

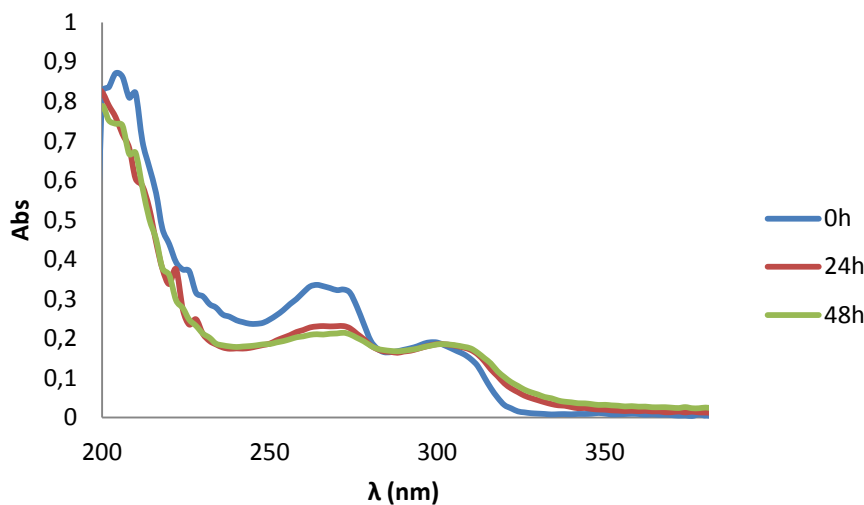**Figure 6:** UV-Visible spectra of a 0.0925 mM solution of **[2]** in methanol at different times.

Figure 7: UV-Visible spectra of a 0.1059 mM solution of **[3]** in methanol at different times.
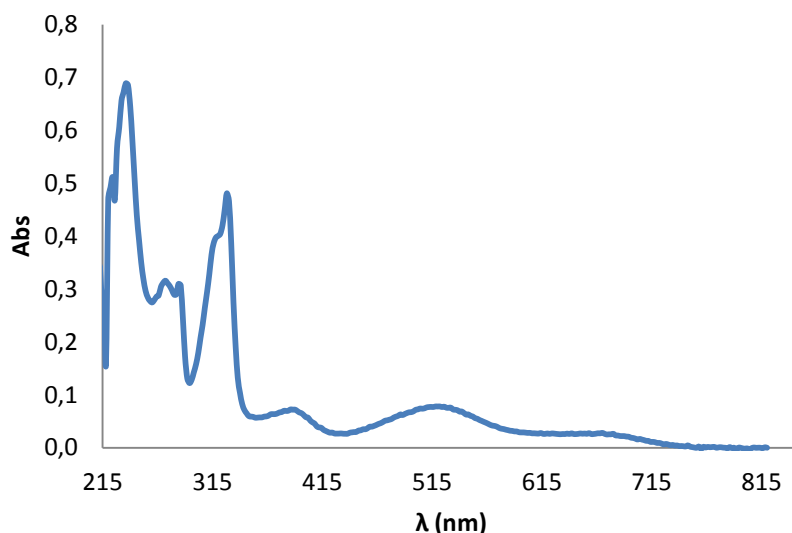
Figure 8: UV-Visible spectra of a 0.124 mM solution of **[4]** in CH₂Cl₂.

4.3 Electrochemical properties and linkage isomerization

Cyclic voltammetry (CV) experiments have been performed to study the redox properties of complexes **[2], [3]** and **[4]**.

For complex **[2],** the CV registered in acetonitrile (Figure 9) exhibits a reversible Ru(III)/Ru(II) redox wave at $E_{1/2}$= 0.77 V. Furthermore, two irreversible redox processes can be observed: an oxidation at $E_{p,a}$= 1.32 V and a reduction at $E_{p,c}$ = 0.58 V. These two irreversible processes are associated with the ligand coordinated to the metal as deduced by comparison with the CV registered for the free ligand (not shown).
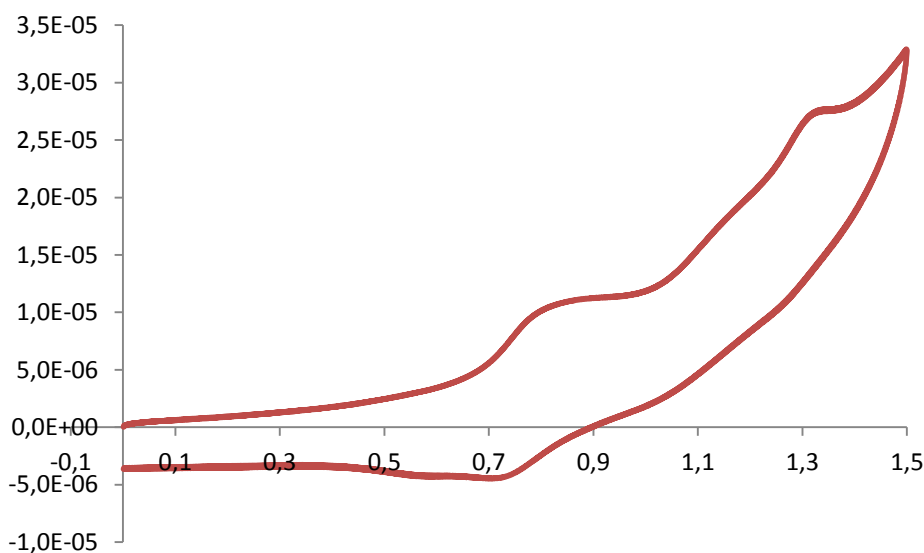

Figure 9: Cyclic voltammogram of **[2]** in CH₃CN + 0.1M TBAH.

17

For complex **[3],** an electrochemically irreversible Ru(III)/Ru(II) redox process is observed at $E_{p,a} = 1.04$ V (figure 10). In addition, two irreversible proces an oxidation at $E_{p,a} = 1.32$ V and a reduction at $E_{p,c} = 0.51$ V are observed too. Comparing the $E_{p,a}$ value with that obtained for **[2]** complex, it can be observed a slight increase in the oxidation potential value for complex **[3]** due to an extra dmso ligand coordinated to the metal that withdraws more electronic density from ruthenium making the oxidation of the metal more difficult. The $E_{p,a}$ value at 1.32 V is also associated with the ligand coordinated to the metal as in complex **[2]**. On the other hand, the irreversible reduction wave at 0.51 V suggests the reduction of the Ru-O_{dmso} species generated after linkage isomerization.
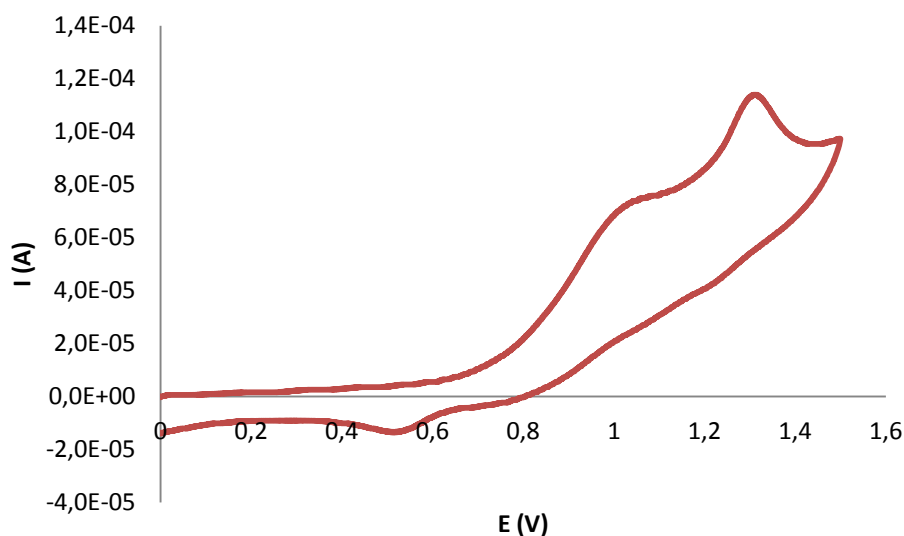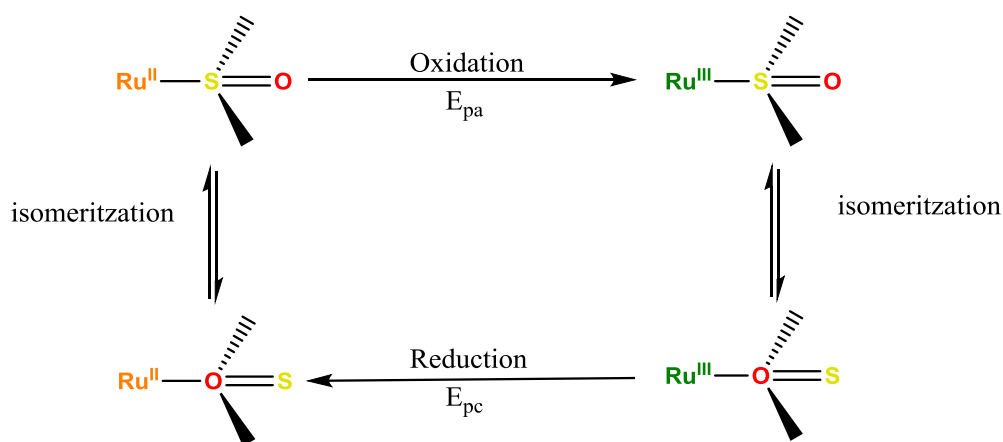

Figure 10: Cyclic voltammogram of **[3]** in CH$_3$CN + 0.1M TBAH.

The linkage isomerization process is shown in Scheme 9. In Ru(II) oxidation state, the dmso ligand is coordinated through S and, after oxidation to Ru(III), the Ru-S $\rightarrow$ Ru-O linkage isomerization takes place. When this species is reduced the dmso ligand returns to the Ru-S form.

Scheme 9: Linkage isomerization process of Ru-dmso complexes.

18

To confirm the linkage isomerization process in complex **[3]**, an additional electrochemical study has been performed. Different cyclic voltammograms have been recorded in acetonitrile at several initial equilibration times, applying an initial potential at $E_{init} = 1.5$ V to oxidize Ru(II) to Ru(III). As it is shown in figure 11, when the equilibration time increases (and therefore the time for oxidation of Ru(II) to Ru(III)) it is observed the decrease of the initial waves that are associate to complex **[3]**. Concurrently there is a new reversible wave at $E_{1/2} = 0.57$ V associated to the complex where a dmso ligand is bonded to the metal through the O atom.
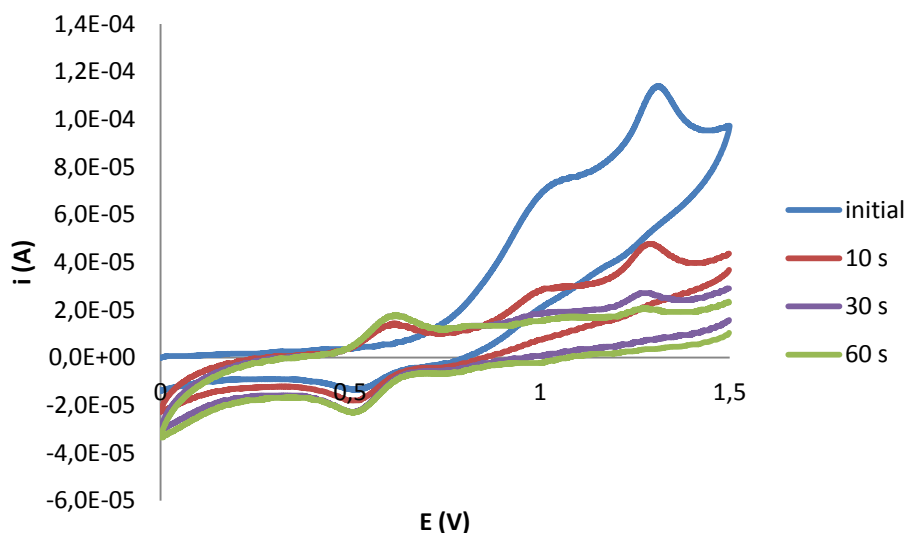

Figure 11: Cyclic voltammograms for **[3]** in CH$_3$CN starting the scanning at $E_{init} = 0$ V (blue) and at $E_{init} = 1.5$ V applying different equilibration times (10, 30 and 60 s).

A similar experiment has been made for complex **[2]** where it was not observed any bond isomerization in the cyclic voltammogram as show in figure 8. The cyclic voltammograms are shown in figure 12 and, as it can be observed, any new wave appears at lower potential than the initial Ru(III)/Ru(II) pair ($E_{1/2} = 0.77$ V) despite applying different equilibration times. Therefore, in this case a bond isomerization doesn't take place. It is observed a new wave at potential about 1.1 V that could be associated to gradual replacement of some ligand (Cl or pzph-OH) by acetonitrile.
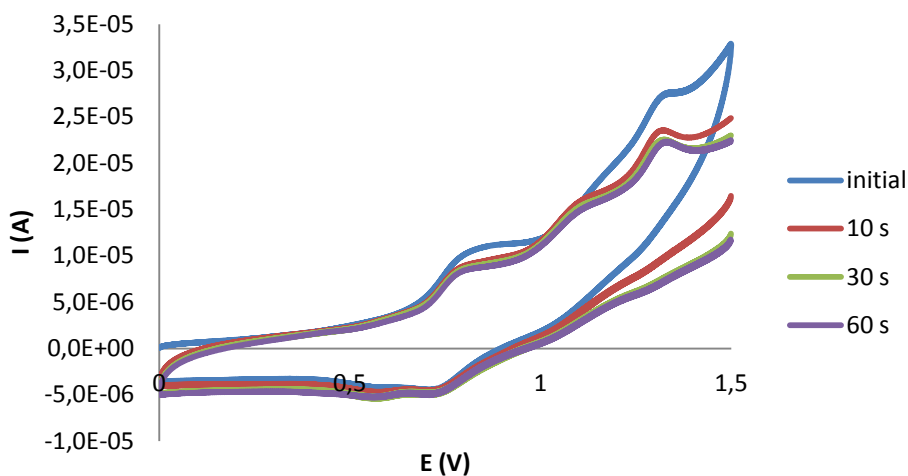

Figure 12: Cyclic voltammograms for **[2]** in CH$_3$CN starting scanning at $E_{init} = 0$ V (blue) and at $E_{init} = 1.5$ V applying different equilibration times (10, 30 and 60 s).

19

The differences between the two complexes could be explained because complex **[3]** has three dmso ligands in facial position. When oxidation of Ru(II) to Ru(III) occurs, more steric hindrance is found because Ru(III) is smaller, probably favoring this isomerization process.

In the case of complex **[4],** the CV registered (figure 13, blue line) exhibits an electrochemically reversible Ru(III)/Ru(II) redox process at $E_{1/2}$ = 0.75 V and a cathodic peak at $E_{p,c}$= 0.40 V which is associated with the product generated by the linkage isomerization process similarly to complex **[3]**.

As mentioned in the section 4.1, when the reaction time to obtain complex **[4]** is longer, it is observed the formation of the *trans*-Cl isomer. It has been performed the cyclic voltammogram of the isomers mixture (red line of figure 13), and it can be observed the wave corresponding to the *trans* isomer at $E_{1/2}$ = 0.94 V.
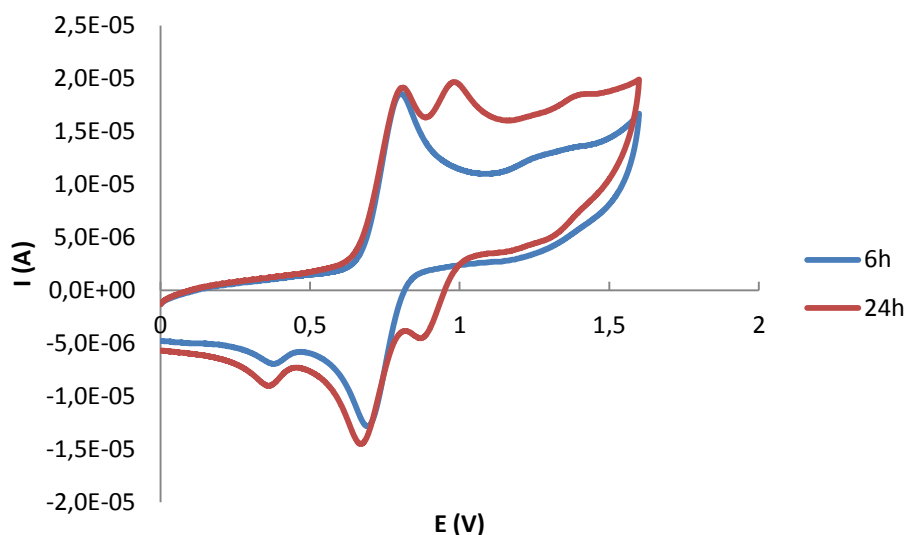

Figure 13: Cyclic voltammogram of **[4]** at different reaction times.

4.5. Catalytic activity for hydration of nitriles

As mentioned above, the hydration of nitriles in order to generate the corresponding amide is an important reaction from both industrial and pharmacological points of view. Traditionally this reaction was carried out in acidic and basic conditions but presented some drawbacks as the formation of by-products such as carboxylic acid. The metal complexes are good candidates as catalysts due to the activation of the CN bond (see Introducction 1.3.1). For this reason, complexes **[3]** and **[4]** have been tested as catalysts in the catalytic hydration process.

This process has been assessed using benzonitrile and acrylonitrile as substrates. The reaction has been performed at 80ºC during 20 h using a ratio 1:100 ([Ru-catalyst]:[substrate]) and water as solvent.

The corresponding amide has been quantified through GC chromatography using biphenyl as the internal standard and finally the hydrolysis product have been analyzed by NMR spectroscopy and compared to pure samples of the corresponding amide to determine the

selectivity of the two complexes as a catalysts. The results of conversion and selectivity values for **[3]** and **[4]** are summarized in table 2.
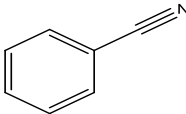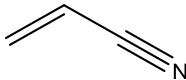
Substrate	[3]		[4]	
	Conv. (%)	Select.(%)	Conv.(%)	Select.(%)
benzonitrile structure	62	>99	89	>99
acrylonitrile structure	40	>99	79	>99

Table 2: Ru-catalyzed hydration of nitriles to amides in water using catalysts **[3]** and **[4]**.

The values obtained in hydration of nitriles (table 2), show an excellent selectivity for both complexes because the carboxylic acid is not found in any case when analyzing the hydrolysis products by NMR spectroscopy. In the case of complex **[3]**, the conversion values for both substrates are moderate, in contrast to the values obtained using **[4]** as a catalyst that shows an excellent conversion to amide in particular for the substrate benzonitrile.

As mentioned above, the catalytic hydration of nitriles involves a substitution process, where a ligand of the complex is replaced by the nitrile and finally there is a nucleophilic attack of hydroxyl anions on the nitrile carbon. The ability of the metal to activate the nitriles is influenced by the electronic characteristics and steric factors of the ligands. The π-acceptor ligands as dmso have a high capacity for withdrawing electron density from the central metal leading to a higher activation of the nitrile.

Comparing the two substrates is interesting to observe that when used benzonitrile as the substrate, higher conversion values than for acrylonitrile are obtained. This may be explained for the resonance delocalization of the aromatic ring that present the benzonitrile, that activates the nucleophilic attack on the nitrile carbon. On the other hand, comparing the two complexes, catalyst **[4]** shows best conversion values. It seems that the electronic factors govern the reactivity because in the one hand, the bulkier (but more activated) substrate works better and in the other hand, the catalyst with the more electron-acceptor ligands (the highly aromatic terpyridine ligand) catalyzes better this reaction. However, the activity of the catalyst will also depend on the ligand in *trans* position to the nitrile. For this reason, more studies should be done to investigate which ligand is replaced by the nitrile and thus elucidate the detailed mechanism.

5. Conclusions

The synthesis and characterization of ruthenium complexes **[2]** and **[3]** with the pzph-OH ligand has been performed. The reaction between **[1]** and pzph-OH lead to two types of complex with one or two pyrazole ligand coordinating in monodentate fashion.

Complexes **[2]** and **[3]** have been characterized by diverse spectroscopic techniques. The NMR spectroscopy has manifested the formation of only one type of isomer in both cases and a complete assignation of the resonances has been possible.

A crystal structure for complex **[2]** has been obtained where the ligand-metal coordination in monodentate form is confirmed. For complex **[3]** this coordination mode can be deduced thanks to elemental analysis, ESI-MS and NMR experiments. Addition of a base to a solution of complex **[3]** presumably leads to a bidentate coordination of the ligand with subsequent oxidation of the ruthenium center and the release of a dmso ligand.

Complex **[4]**, with the trpy ligand, has been synthesized and characterized. The ^{1}H-NMR has manifested the formation of only type of isomer when the reaction is maintained for 6 hours. However, the formation of another isomer is observed for 24 h refluxing time.

The UV-Vis spectroscopy for the three complexes has been performed. The spectra show MLCT and intraligand π-π* transitions in all cases, that are of lower energy for complex **[4]** when compared to **[2]** and **[3]**, due to the higher aromatic character of the trpy ligand with regard to pzph-OH. For complexes **[2]** and [**3**] an evolution of the UV-vis bands is observed possibly due to an exchange one ligand by methanol.

Complexes **[2]**, **[3]** and **[4]** have been characterized by electrochemical techniques. For complexes **[2]** and **[4]** reversible redox waves corresponding to the Ru(III)/Ru(II) redox pair are observed whereas complex **[3]** displays an irreversible oxidation process due to linkage isomerization of a coordinated dmso. The linkage isomerization has been confirmed for **[3]** through cyclic voltammograms performed at different initial equilibration times. Complex **[4]** also experiences dmso linkage isomerization as manifested by an additional cathodic peak observed in the cyclic voltammogram.

Complexes **[3]** and **[4]** have been evaluated as catalyst in the hydration of nitriles in neutral conditions using water as a solvent for benzonitrile and acrylonitrile as substrates. The conversions displayed by complex **[4]** are better than those of complex **[3]**, but both complexes achieve excellent selectivities for the amide product. The catalytic process seems to be governed by electronic factors because the bulkier, but more activated, benzonitrile substrate displays better conversions than the smaller acrylonitrile for both catalysts, and complex **[4]**, with more electron-withdrawing ligands, displays also better conversions.

6. References

[1] (a)Ballardini, R.; Balzani, V,; Credi, A.; Gandolfi, M. T.; Venturi, M. *Int. J. Photoenergy* **2004**, *6,*1. (b) Baranoff, E.; Collin, J. P.; Furusho, J.; Furusho, Y.; Laemmel, A.; Sauvage, J.P. *Inorg. Chem.* **2002**, *41*,1215.

[2] Qu, P.; Thompson, D. W.; Meyer, G. J. *Langmuir* **2000**, *16*, 4662.

[3] Butler, J.; George, M.; Schoonover, J.; Dattelbaum, D.; Meyer, T. *Coord. Chem. Rev*. **2007**, *251*, 492.

[4] Seok, W. K.; Meyer, T. J. *Inorg. Chem.* **2005**, *44*, 3931.

[5] Ley, S. V.; Norman, J.; Griffith, W. P.; Marsden, S. P. *Synthesis* **1994**, *7*, 639.

[6] Coe, B. J. *Coord. Chem. Rev*. **2013**, *257*, 1438.

[7] Mikuriya, M.; Yoshioka, D.; Handa, M. *Coord. Chem. Rev*. **2006**, *250*, 2194.

[8] Fillaut, J.; Andriès, J.; Marwaha, R. D.; Lanoë, P.; Lohio, O.; Toupet, L.; Gareth Williams, J. *J. Organomet. Chem.* **2008**, *693*, 228.

[9] Yoshida, J.; Watanabe, G.; Kakizawa, K.; Kawabata, Y.; Yuge, H. *Inorg. Chem.* **2013**, *52*, 11042.

[10] Zhang, S.; Ding, Y.; Wei, H. *Molecules* **2014**, *19*, 11933.

[11] Belser, P.; De Cola, L.; Hartl, F.; Adamo, V.; Bozic, B.; Chriqui, Y.; Iyer, V. M.; Jukes, R. T. F.; Kühni, J.; Querol, M.; Roma, S.; Salluce, N. *Adv. Funct. Mater*. **2006**, *16*, 195.

[12] Delaney, S.; Pascaly, M.; Bhattacharya, P. K.; Han, K.; Barton, J. K. *Inorg. Chem.* **2002**, *41*, 1966.

[13] Cotton, F. A.; Francis, R. *J. Inorg. Nucl. Chem.* **1961**, *17*, 62.

[14] Mola, J.; Romero, I.; Rodríguez, M.; Bozoglian, F.; Poater, A.; Sola, M.; Parella, T.; Benet-Buchholz, J. *Inorg. Chem.* **2007**, *46*, 10707.

[15] Wang, L.; Duan, L.; Stewart, B.; Pu, M.; Liu, J.; Privalov, T.; Sun, L. *J. Am. Chem. Soc.* **2012**, *134*, 18868.

[16] a) Sava, G.; Pacor, S.; Mestroni, G.; Alessio, E. *Clin. Exp. Metastasis* **1992**, *10*, 273. b) Bratsos, L.; Jedner, S.; Gianferrara,T.; Alessio, E. Chimia. **2007**, *61*, 692.

[17] Komiya, S.; Susuki, S.; Watanabe, K.; *Bull. Chem. Soc. Jpn.* **1971**, *44*, 1440.

[18] W.K. Fung, X. Huang, M.L. Man, S.M. Ng, M.Y. Hung, Z. Lin, C.P. Lau, *J. Am. Chem. Soc.* **2003**, *125*, 11539.

[19] (a) Murahashi, S.I.; Sasao, S.; Saito, E.; Naota T. *J. Org. Chem.* **1992**, *57*, 2521. (b) Murahashi, S.I.; Sasao, S.; Saito, E.; Naota T. *Tetrahedron* **1993**, *49*, 8805.

[20] (a) Ghaffar, T.; Parkins. A. W. *Tetrahedron Lett*. **1995**, *36*, 8657. (b) Akisanya, J.; Parkins, A. W.; Steed, J. W. *Org. Process Res. Dev*. **1998**, *2*, 274.

[21] Oshiki, T.; Yamashita, H.; Sawada, K.; Utsunomiya, M.; Takahashi, K.; Takai, K. *Organometallics* **2005**, *24*, 6287.

[22] Goto, A.; Endo, K.; Saito, S. *Angew. Chem. Int. Ed.* **2008**, *47*, 3607.

23 (a) Cadierno, V.; Francos, J.; Gimeno, J.; *Chem. Eur. J.* **2008**, *14*, 6601; (b) Cadierno, V.; Diez, J.; Francos, J.; Gimeno, J. C*hem. Eur. J.* **2010**, *16*, 9808.

24 Ferrer, Í.; Rich, J.; Fontrodona, X.; Rodríguez, M.; Romero, I. *Dalton Trans.* **2013**, *42*, 13461.

25 Bruker Advanced X-ray Solutions. SMART: Version 5.631, 1997-2002.

26 Bruker Advanced X-ray Solutions. SAINT +, Version 6.36A, 2001.

27 G. M. Sheldrick, *Empirical Absorption Correction Program*, Universität Göttingen, 1996 Bruker Advanced X-ray Solutions. SADABS Version 2.10, 2001.

28 G. M. Sheldrick, *Program for Crystal Structure Refinement*, Universität Göttingen, 1997. Bruker Advanced X-ray Solutions. SHELXTL Version 6.14, 2000-2003. SHELXL-2013 (Sheldrick, 2013).

29 Catalán, J.; Fabero, F.; Claramunt, R. M.; Santa Maria, M. D.; Foces-Foces, M. C.; Hernández Cano, F.; Martínez-Ripoll, M.; Elguero, J.; Sastre, R. *J. Am. Chem. Soc.* **1992**, *114*, 5039.

30 (a) Evans, I. P.; Spencer, A.; Wilkinson, J.J; *J. Chem. Soc., Dalton Trans.* **1973**, *2*, 204; (b) Alessio, E.; Iengo, E.; Zorzet, S.; Bergamo, A.; Coluccia, M.; Boccarelli, A.; G. J. J. Sava. *G. J. Inorg. Biochem.* **2000**, *79*, 137.

31 Ziessel, R.; Grosshenny, V.; Hissler, M.; Stroh, C. *Inorg. Chem.* **2004**, *43*, 4262.

32 Sens, C.; Rodríguez, M.; Romero, I.; Llobet, A.; Parella, T.; Sullivan, B. P.; Benet-

Buchholz, J. *Inorg. Chem.* **2003**, *42*, 2040.